Military Technical College
Kobry El-kobbah,
Cairo, Egypt

5th International Conference
on Electrical Engineering
ICEENG 2006

AIRCRAFT RECOGNITION BASED ON
ISODENSITY AND ORDINARY MOMENTS

AA Somaie

Abstract

The ability to extract and describe the salient features represents the most difficult task of the aircraft recognition systems. In this paper, an aircraft recognition system based on the isodensity lines associated with the three-dimensional reflectivity of the model is illustrated. A recognition algorithm is described, which uses combination of 2-D moments in three-dimensional isodensity maps to represent the aircraft as a feature vector containing $2L$ elements. Using a distance-weighted k-nearest neighbour rule as a classifier, the algorithm achieves a highly recognition rate when applied to 336 test images that represent six aircraft models. The same procedures are applied using the first two components of invariant moments, and the first system was found superior to this system with about 15% using the same number of isodensity lines.

Key words: Image processing, moment, pattern recognition, computer vision.

I Introduction

Research on image recognition systems continues because these systems are useful tools in many applications, such as criminal identification, security checking, video surveillance, and target tracking. Aircraft recognition systems are commonly utilize in different manner as a feature vector or 2-D perspective views.

Several recognition systems used the Fourier descriptors and 2-D moments to recognize the objects in 2-D and 3-D planes. Granlund [1] is one example of a researcher who presented a method to extract new features from Fourier coefficients used as shape descriptors invariant with respect to size, orientation, position, and starting conditions. Dudani [2] presented an experimental study using the theory of 2-D moment invariants [3] for automatic identification of 3-D objects from 2-D perspective views. In his study, a Bayes rule and a distance-weighted k-nearest neighbour rule are applied separately for the design of an aircraft recognition system.

_____

*Egyptian Armed Forces, aaisomaia@yahoo.com
University of Calgary, Department of Electrical and Computer Engineering, Calgary, Canada.

Other recognition systems use the grey-scale digitized image of an aircraft directly without pre-processing operations such as segmentation and these include some well known systems such as WISARD, back propagation networks and Kohonen's matrix system, all of which are reviewed in reference [4]. Somaie et al used the back propagation network to recognize aircrafts [5]. In this paper, the presented training algorithms satisfied high recognition performance when the number of hidden neurons was less than or equal ten times the number of classes. It was found that the network recognizes the test images correctly even the noisy and the incomplete images [5]. An information theory approach has been exploited by Somaie et al [6], who used eigencrafts (in a low dimensional space) to model aircrafts and to distinguish them in a limited database of aircrafts. Somaie et al exploited the principal component analysis to create a new co-ordinate system called eigencraft for object representation where each aircraft is projected onto that plane and the projection coefficients are used for the recognition purpose. The new features are invariant to translation, scale and rotation.

The approach described in this paper is based on isodensity maps and uses a simple method of clipping the image from the background together with a fast moment-based recognition algorithm. An isodensity line approach may be better able to cope with problems caused by aircraft maneuvers because these lines contain some information about the shape of the aircraft fuselage from the nose to the tail.

The procedures used to capture aircraft images and to isolate an aircraft from the background and generate an isodensity map of aircraft are described in section II. 2-D moments are used to form a feature vector and these, together with the recognition algorithm, are defined in section III. The complete recognition system has been tested using a variety of aircraft images and some of the experimental results obtained are presented in section IV. Section V contains discussion and conclusions.

II Isodensity map of an aircraft

Individual models of aircrafts were illuminated using a white spotlight, of power 150 W with reflector of diameter 28 cm. A fixed working distance was used during image capture process. A frame transfer type CCD camera model 4712 (625 line CCIR standard), manufactured by COHU and fitted with a f/1.4 Cosmicar TV lens of 25mm focal length, was used for image capture. This combination of focal length, camera and working distance ensured that even the longest aircraft captured occupied no more than 90% of the vertical field of view. The camera was connected to a PIP1024 frame grabber, manufactured by Matrox, which occupied one of the expansion slots of a 0.996 GHz, 128 MB of RAM, Pentium III PC. All images were digitized to 256 grey levels and were 512 by 512 pixels in size. To make it easier to isolate the aircraft from the background, each model was put at a black sheet prior to image capture. Eight separate images were captured for each aircraft model in $\cong n\pi/4$ degree ($n = 0,1,...,7$) to get different orientation of the aircrafts. Fig. 1 shows samples of aircraft images after aspect ratio correction.

The following steps were taken to clip each aircraft image from the background and to centralize the aircraft into the image plane.

(1) An aspect ratio correction was first carried out using bilinear interpolation.

(2) Smoothing was performed using a median filter with a window of size 5 by 5 pixels, which yielded an image named "image 1".

(3) A binary image map was obtained by thresholding. If image1>= threshold value, image2=225, else image2 = 0.

(4) If the image called "image 3" is set to be '0' grey level, then the clipped image can be extracted simply, if image2 = 255, then image3 = image1.

(5) The centre of gravity of each aircraft was obtained, and each aircraft was translated to the centre of the image plane.
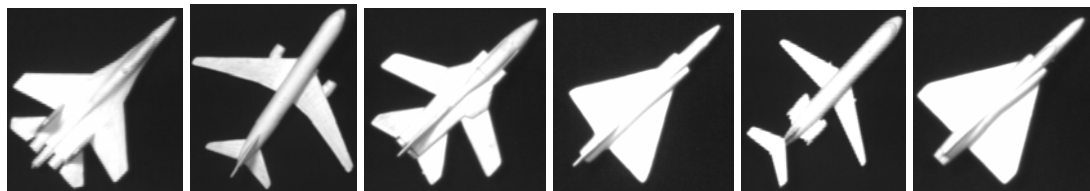

Fig. 1. Samples of the aircraft images after aspect ratio correction.

The entire process of image segmentation is illustrated in Fig. 2 (a) to (c) which shows an example of the aircraft image after aspect ratio correction, the binary image, and the clipped aircraft image respectively.
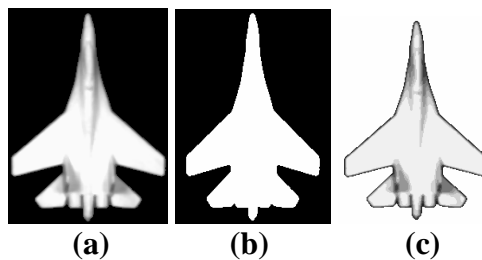

(a)   **(b)**   **(c)**

Fig. 2. (a) Aircraft image after aspect ratio correction, (b) the binary image, and (C) the corresponding aircraft clipped from the background.

Once the aircraft was isolated from its background, the isodensity map of each aircraft was obtained using the following processing.

(1) Calculate the histogram of the clipped aircraft.

Proceedings of the 5th ICEENG Conference, 16-18 May, 2006 | |

(2) The grey range of the histogram is then divided into *L* equal levels, where the range of each level or band is defined precisely.

(3) A number of *L* isodensity lines were obtained to each aircraft. Each isodensity line was represented in 2-D plane as a binary image where the background is set to zero grey level and the isodensity region was replaced by the corresponding value of *L*.

(4) The isodensity map of aircraft was constructed by adding their isodensity *L* regions into one image.

Fig. 3 illustrates the processing of constructing of the isodensity map, where Fig. 3 (a) to (c) shows the histogram of the clipped aircraft, the histogram of the isodensity regions, and the isodensity map respectively.
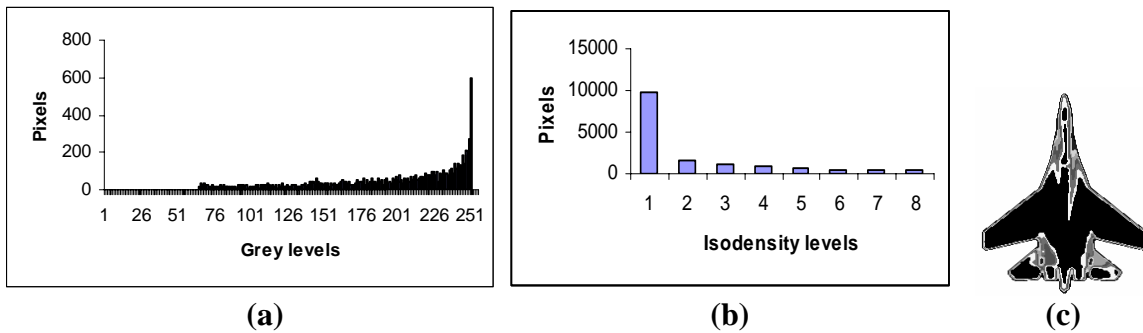

(a)   **(b)**   **(c)**

Fig. 3. (a) The grey-level histogram of one of an aircraft image, (b) the corresponding quantized histogram, and (c) the isodensity aircraft map.

The isodensity map (contrast stretched and magnified for display purposes) obtained from the aircraft of Fig. 2(C) using the value *L* = 8 is presented in Fig. 3. The isodensity map emphasises the variation of reflectivity resulting from variations in aircraft fuselage condition and orientation over the aircraft image. The isodensity regions of the isodensity aircraft map depicted in Fig. 3 (c) for each of the isodensity band are shown in Fig. 4.
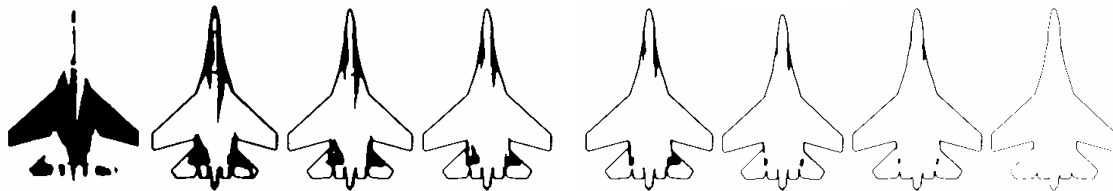

Fig. 4. From left to right isodensity regions of the isodensity map depicted in Fig. 3 (c).

Proceedings of the 5th ICEENG Conference, 16-18 May, 2006

III The recognition algorithm

2-D moments [3] have been used as the basis of feature vectors in many pattern recognition applications and are defined as

$$m_{pq} = \sum_x \sum_y f(x, y) x^p y^q \tag{1}$$

Where $(p + q)$ is the order of the moment defined for p, $q = 0, 1, 2, ...,$ and $f(x, y)$ is the 2-D intensity function of the pixel with co-ordinates (x, y). It is clear that equation (1) is not invariant under changes of position, scale, and orientation of the image. A more useful set of moments are the central moments $\overline{m}_{pq}$ defined as

$$\overline{m}_{pq} = \sum_x \sum_y (x - \overline{x})^p (y - \overline{y})^q f(x, y), \tag{2}$$

where $\overline{x} = m_{10} / m_{00}$, and $\overline{y} = m_{01} / m_{00}$. The set of moments in equation (2) are invariant to translation, but not scale, and orientation. In reference [3], Hu presented a set of moments, which are combinations of the central moments $\overline{m}_{pq}$. The basic idea to achieve scale invariance is to divide each component of the set $\{\overline{m}_{pq}\}$ by the factor equal $(m_{00})^{(\frac{p+q}{2})+1}$ to get a dimensionless moment set. Hu then defined combinations [3] of $[\overline{m}_{pq} / (m_{00})^{(\frac{p+q}{2})+1}]$ which are invariant to translation, scale, and orientation. The set of moments defined by Hu consists of seven elements derived from the second and the third moments of the set $\{\overline{m}_{pq}\}$. Although using these moments can compensate for yaw rotations about the aerodynamic axis left or right in the x-y plane, they cannot compensate for other rotations occurring in the aircraft maneuvers such as rotation of the aircraft's head about the longitudinal axis (roll or bank rotation) or pitching the nose up or down about the wing axis. The first and the second element of the 2-D invariant moment set are the most commonly used elements and used by Hu [3] for character representation. These elements are defined as

$$(\overline{m}_{20} + \overline{m}_{02})/m_{00}^2, \text{ and} \tag{3}$$

$$[(\overline{m}_{20} - \overline{m}_{02})^2 + 4\overline{m}_{11}^2]/m_{00}^4 \tag{4}$$

The equation (2) is invariant to translation, and not to scale or rotation. Since all the aircraft images were captured under nominally the same conditions, the sensitivity of $\overline{m}_{pq}$ to changes of scale should not be very significant because the distance between camera and model was kept constant. Changing orientation of the aircraft is still one of the most difficult problems for an aircraft identification system but again in the present work the camera system was viewed each model from its plane view. In this paper, the following combinations of the $\overline{m}_{pq}$ calculated using individual isodensity regions have been used to form a feature vector of each aircraft for recognition purposes.

$$m_1 = m_{oo} = \sum_x \sum_y f(x, y) \qquad \text{, and} \qquad (5)$$

$$m_2 = (\overline{m}_{20} + \overline{m}_{02}) / m_{00} \qquad (6)$$

Since equation (5) represents the area of each isodensity region, and equation (6) contains the same combination as equation (3), equations (5) and (6) are invariant to the translation and rotation (if the rotation is in *x-y* plane). Scale invariance can be achieved easily, if the clipped aircraft images are normalized using the same manner like Khotanzad method [7]. However, the present application does not need this normalization, since the camera position is fixed. Disadvantages of normalizing are that this process will add computation noise as well as possibly changing the contrast of the new images.

The combinations defined by equations (5) and (6) were calculated for each of the *L* isodensity regions with *f(x, y)* replaced by the corresponding value of *L*. This provided a feature vector of dimension 2*L* to replace the aircraft image for recognition purposes. The selection of the classifier for any pattern should be appropriate to the problem in hand and for this algorithm the distance-weighted k-nearest neighbour rule was preferred because the probability of error is small, compared with other classifiers and, unlike a Bayes classifier [8], it does not need any a priori information. The entries in the database of the aircraft library are represented by $R_j(i)$, where $i = 1, 2 , ..., 2L$ and $j = 1, 2, ..., K$, where K is the number of aircrafts. If $T(i)$ represents the unknown pattern, then the distance between $T(i)$ and each entry in the library $R_j(i)$ can be defined as

$$d_j = [(T(j) - R_j(t))^2]^{1/2} \qquad (7)$$

If d_{min} represents the minimum distance found, corresponding to the nearest neighbour and d_{max} represents the maximum distance found, and then a weight w_j related to each library entry can be defined as follows:

$$w_j = \frac{d_{max} - d_j}{d_{max} - d_{min}} \qquad (8)$$

It is clear that the value of w_j varies from the maximum value 1 for the nearest neighbour to a minimum value of 0 for the furthest neighbour.

V Experimental results

A six aircraft models were used for this study included different aircrafts Eight snapshots were taken of each model under nominally the same conditions and one version of each of these models was used as a reference pattern while the other seven versions were used as test patterns, giving 336 different test permutations.

The performance of the recognition system was tested using one set of m_1 and m_2 values. This set of the feature vector used to recognize the aircraft and the corresponding recognition obtained for different values of L are shown in the first row of Table 1. It can be seen that at first the performance increases as L increases and becomes stable at a value of 100% when $L \geq 4$.

It was found that the identification failures were usually associated with boundary variations in the aircraft image of a given model due to changes in the orientation between settings. The second method was carried out after replacing the combined moments defined by equations (5) and (6) with a 2-D invariant moments defined by equations (3) and (4) and the recognition performance is illustrated in the second row of the Table 1. It is apparent from Table 1 that the best recognition rate achievable was 85.7% with $L = 8$ which is significantly worse than those presented in Table 1 (row 1) as shown in Fig. 5. In order to improve the recognition performance listed in Table 1 (row 2), the feature vectors defined by equations (3) and (4) are normalized as follow,

$$\overline{m}_k(i) = (m_k(i) - \mu_i)/\sigma_i, \qquad\qquad (9)$$

where μ_i and σ_i represent the mean and the standard deviation of component i of the feature vectors belonging to the aircraft library, and $k = 1, 2, ..., K$, where K is the number of classes or aircrafts. Since each aircraft in the aircraft library has been normalised using equation (9), each component of the feature vectors has zero mean, and unit variance. At the recognition stage, each unknown vector should normalize before applying to the classifier, and the recognition success was found to achieve 93.4% using only twelve components as shown in Table 2 and Fig. 6. It was found if the same normalization is applied to the feature vectors defined by equations (5) and (6), it does not add any significant effect as shown in Fig. 6. It is apparent from Fig. 6 that it is still the aircraft identification system based on the 2-D combination moments defined by equations (5) and (6) is superior than that one using the first two components of the invariant moments set.

L	2	4	6	8	10	12	14
IMR (%)	97.9	100	100	100	100	100	100
OMR (%)	73.3	84.2	85.4	85.7	86.6	86.0	84.8

Table 1. Recognition rates for the aircraft using isodensity and ordinary moments.

L	2	4	6	8	10	12	14
IMR (%)	97.6	100	99.4	99.7	99.7	99.7	100
OMR (%)	91.0	93.1	93.4	91.9	91.6	92.8	91.9

Table 2. Recognition rates for the aircrafts using a normalized feature vector.
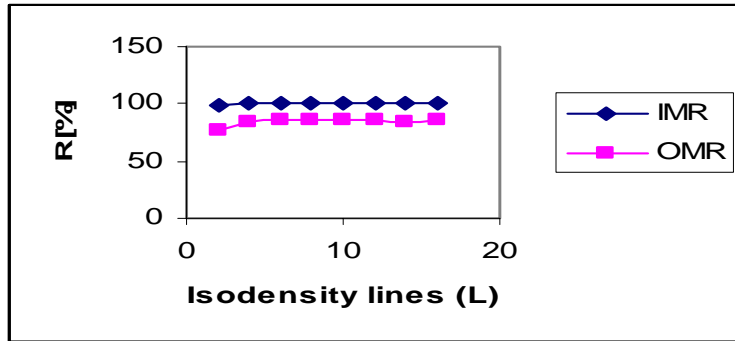

Fig. 5. The top curve represents the performance of the aircraft identification system using equations (5) and (6) as a feature vector and the lower curve corresponds to the same system using equations (3) and (4).
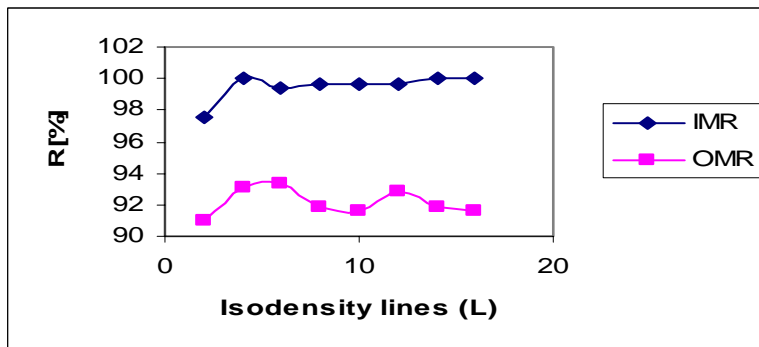

Fig. 6. The top curve represents the performance of the aircraft identification system using equations (5) and (6) as a feature vector and the lower curve corresponds to that same system using equations (3) and (4) after normalization using equation (9).

　The recognition success rate using both methods depends also on the dynamic range of the isodensity map. In other words, if the dynamic range of the iosdensity maps is increased for the

case in hand, the optimum recognition performance could move towards the right along the *L* axis.

VI Discussion and conclusions

The main task of the most recognition systems is to reduce the dimensionality of the input pattern, which in turn speeds up the process of the target identification. The system described in this paper scores well on this count because it employs a feature vector consisting of at most only 16 components. The presented recognition algorithm was found to achieve a 100% recognition rate when applied to 336 test images taken from six aircraft models, which were available at that time. A further advantage of the present technique is the very short recognition time required because of the low dimensionality of the aircraft data.

It is found that as combination of 2-D isodensity moments are replaced by the first two components of the invariant moments set and the resulting recognition rate was found to be only 85.7%. These results improved when the feature vector was normalised, achieving 93.4% using a 12-dimensional feature vector. On the other hand, this normalization does not make any significant difference in the first method. However, the effect of changing the combination of isodensity 2-D moments from first and second orders to higher orders may not be useful because the later are more sensitive to the noise than the lower order moments. In conclusion, it was gratifying to find that the present aircraft identification system achieved a 100% recognition rate when applied to a number of models chosen randomly. Nevertheless, further investigations need to be carried out to determine how well the recognition rate holds up as the number of models increases.

Acknowledgment

References

[1] G. H. Granlund, Fourier Recognition for Hand Print Character Recognition, IEEE Trans. on Computers, PP. 195-197, February (1972).
[2] Sahibsingh A. Dudani, Kenneth J. Breeding, and Robert B. Mcghee, Aircraft Identification by Moment Invariants, IEEE Trans. on Computers, Vol. 2-26, No. 1, PP. 39-45, January, (1977).
[3] M. Hu, Visual Pattern Recognition by Moment Invariants, IRE Transactions on Information Theory. Vol. IT-8, pp. 179-187, February (1962).
[4] T. Agui, Y. Kokubo, H. Nagahashi and T. Nagao, Extraction of Face Region from Monochromatic Photographs Using Neural Networks, Proceedings of the Second International Conference on Automation, Robotics and Computer Vision, Vol. 1, pp. CV-18.8.1-CV-18.8.5, Singapore, September (1992)

[5] Somaie A.A., Badr A. and Salah T., Aircraft image recognition using back-propagation Proceedings of the Radar, 2001 CIE International, IEEE Conference Proceedings ,PP. 498 – 501, 15-18 October, China, Beijing, (2001).

[6] Somaie A.A., Badr A. and Salah T., Aircraft recognition system using eigenvector technique Proceedings of the Sixteenth National Radio Science Conference, NRSC, IEEE Conference Proceedings, PP. C29/1 - C29/9, 23-25 February, Egypt, Cairo, (1999).

[7] Alireza Khotanzad and Yaw Hua Hong, Invariant Image Recognition by Zernike Moments, IEEE Trans. on Pattern Analysis and Machine Intelligence, Vol. 12, No. 5, PP. 489-497, May, (1990).

[8] T. M. Cover, Nearest Neighbour Pattern Classification, IEEE Transactions on Information Theory. Vol. IT-13, pp. 21-27, January (1967).